Study of the Perturbation Series for the Ground State of a Many-Fermion System. II*

GEORGE A. BAKER, JR., B. J. HILL, AND ROBERT J. MCKEE, JR.
University of California, Los Alamos Scientific Laboratory, Los Alamos, New Mexico
(Received 19 March 1964)

We derive through fourth order in the potential strength the many-fermion perturbation series for a velocity-dependent force which exactly simulates, in two-body scattering, a hard core. We use the Padé approximant method to sum the complete series and the ladder and Brueckner approximation series. We compare these results with those of the K-matrix procedure and find that the K-matrix procedure fails to converge for the Brueckner approximation in the only interesting region. We also investigate near saturation, a system something like He^3. We find that there is not, as some have speculated, a magic cancellation that would cause the ring diagrams to be of little importance there.

I. INTRODUCTION

IN this paper we extend the study of the many-body perturbation series which we began in our previous paper.[1] In that paper we studied the accuracy of the ladder and Brueckner approximations both as a sum of a set of diagrams and as they are computed in practice, for the soft repulsive, square-well potential. In this paper we extend our study to a velocity-dependent force which exactly simulates a hard core for two-body scattering and also to this force plus an ordinary attractive force. For the "hard-core" velocity-dependent force, both the ladder and Brueckner approximations (as a set of diagrams) are satisfactory for low to moderate densities. For high densities the Brueckner approximation is still good, but the ladder approximation is appreciably less good. However, the Brueckner approximation, as ordinarily calculated, does not converge for these densities and so as a practical matter is no better than the ladder approximation.

In our previous paper (I) we pointed out that some have suggested that near equilibrium, the ring diagrams, which we found to be quite important for the repulsive square-well, may not be nearly so important. We have investigated this point in Sec. IV and find that, for a case somewhat similar to He^3, the ring diagrams are just about as important as they were for the other cases investigated.

In the second section of our paper we derive the first four terms of the perturbation series in the potential strength for the "hard-core" velocity-dependent force and evaluate them at several densities. In the third section we prove that certain Padé approximants form rigorous upper and lower bounds to the energy in ladder approximation. We then use the Padé approximants to sum the complete series, the ladder approximation series, and the Brueckner approximation series. An interesting comparison is made, in ladder approximation, with the result from our previous paper for an actual hard-core force as a function of density.

In the fourth section we repeat the procedure of the second and third sections for a "hard-core" velocity-dependent force plus an attractive force.

II. LOW-ORDER PERTURBATION SERIES TERMS

For two-body scattering, it is possible to simulate a hard core exactly by use of a nonsingular velocity-dependent force.[2] Let $\mu(r)$ be greater than or equal to one and $\mu(\infty)=1$. Then, if Λ is Legendre's operator with eigenvalues $l(l+1)$,

$$v=-\{[\mu(r)-1]\nabla^2+\nabla\mu\cdot\nabla+\tfrac{1}{4}\nabla^2\mu+\{\mu r^{-2}-[\rho(r)+a]^{-2}\}\Lambda-\tfrac{1}{2}\mu'[\mu'/(8\mu)-r^{-1}]\} \quad (2.1)$$

exactly simulates a hard core of radius

$$a=\int_0^\infty\{1-[\mu(r)]^{-1/2}\}dr, \quad (2.2)$$

where

$$\rho(r)=\int_0^r[\mu(r)]^{-1/2}dr. \quad (2.3)$$

This force does not, of course, exactly simulate a hard core in the many-body problem except in the limit of zero density where only binary collisions are important.

We have selected, for convenience in these calculations,

$$\mu(r)=1+se^{-r/\beta},\qquad s=(2e^{0.5}-1)^2-1=4.2782422, \quad (2.4)$$

which implies $a=\beta$. In momentum representation the matrix elements of this potential are

$$\langle\nu\mathfrak{y}|v|\lambda\eta\rangle=\frac{\beta\delta(\lambda+\eta,\nu+\mathfrak{y})}{\Omega}\left\{\frac{2\pi s(\beta q_{\rm exch})^2}{[1+(\beta q)^2]^2}+\frac{2\pi s}{1+(\beta q)^2}+\frac{\pi}{4}\Theta(q)-4\pi[(\beta q_{\rm exch})^2-(\beta q)^2]\Phi_0(q)-4\pi[-(\beta q)^2+(\beta q_{\rm exch})^2P_2(\cos\theta)]\Phi_2(q)\right\}, \quad (2.5)$$

* Work performed under the auspices of the U. S. Atomic Energy Commission.

[1] G. A. Baker, Jr., J. L. Gammel, and B. J. Hill, Phys. Rev. 132, 1373 (1963). We shall call this work paper I hereinafter.

[2] G. A. Baker, Jr., Phys. Rev. 128, 1485 (1962).

where

$$\Theta(q)=\frac{s^2}{q\beta^3}\int_0^\infty rdr\,\sin rq e^{-2r/\beta}(1+se^{-r/\beta})^{-1}, \tag{2.6}$$

$$\Phi_k(q)=\frac{1}{6\beta^3}\int_0^\infty r^2dr\left\{\mu(r)-\frac{r^2}{[\rho(r)+a]^2}\right\}j_k(rq), \tag{2.7}$$

$$q=\tfrac{1}{2}|\mathfrak{y}+\mathfrak{x}-\mathfrak{v}-\boldsymbol{\eta}|, \quad q_{\text{exch}}=\tfrac{1}{2}|\mathfrak{y}+\boldsymbol{\eta}-\mathfrak{v}-\mathfrak{x}|, \tag{2.8}$$

Ω is the (large) volume of the confining box, θ is the angle between $\mathbf{q}$ and $\mathbf{q}_{\text{exch}}$, and $\delta(\mathbf{x},\mathbf{y})$ the Kronecker delta function.

We have calculated all the terms through fourth order in the interaction potential in the Goldstone[3] expansion of the ground-state energy of a system of spin-$\frac{1}{2}$ fermions. Investigation of velocity-dependent forces in perturbation theory have been made through second order in the nuclear case by Green,[4] and Da Providenca.[5]

We proceed substantially as we did in paper I; and we refer the reader to that paper for a detailed description of our procedures. We discuss here only the differences between the present calculation and the previous ones. The differences arise from the fact that the potential now depends, not only on the momentum transfer as it did before, but also on the exchanged momentum transfer and the square of the cosine of the angle between these two momenta. In order to save computer time, we have approximated the functions Θ and Φ_k by some simple expressions which we have listed in the Appendix and which are usually accurate to a few hundredths of a percent.

If we denote the potential by $v(\mathbf{q}/k_F\beta,\mathbf{q}_{\text{exch}}/k_F\beta)$ then the first-order contribution is

$$3(k_F\beta)^3/(2^5\pi^4)\int_{|\mathbf{m}|\le1,|\mathbf{n}|\le1}d\mathbf{m}d\mathbf{n}\times\{v[0,(\mathbf{m}-\mathbf{n})]-\tfrac{1}{2}v[(\mathbf{m}-\mathbf{n}),0]\}, \tag{2.9}$$

which can be partially done analytically as

$$(3/\pi)\{(2/9)[\tfrac{1}{2}s+\tfrac{1}{16}\Theta(0)](k_F\beta)^3+(4/15)[\tfrac{1}{2}s+\Phi_0(0)](k_F\beta)^5+\int_0^{2k_F\beta}K^2dK\left[\frac{2}{3}-\frac{1}{2}\left(\frac{K}{k_F\beta}\right)+\frac{1}{24}\left(\frac{K}{k_F\beta}\right)^3\right](K^2/2)[\Phi_0(K/\beta)+\Phi_2(K/\beta)]-\Theta(K/\beta)/32-\tfrac{1}{4}s/(1+K^2)\}. \tag{2.10}$$

The second-order contribution is

$$-3(k_F\beta)^4/(2^{11}\pi^{10})\int\frac{d\mathbf{m}d\mathbf{n}d\mathbf{q}v(\mathbf{q},\mathbf{m}-\mathbf{n}+\mathbf{q})[v(\mathbf{q},\mathbf{m}-\mathbf{n}+\mathbf{q})-\tfrac{1}{2}v(\mathbf{m}-\mathbf{n}+\mathbf{q},\mathbf{q})]}{q^2+\mathbf{q}\cdot(\mathbf{m}-\mathbf{n})}, \tag{2.11}$$

where the integration is carried out over all values allowed by the Pauli exclusion principle.

For the third-order contributions we may simply replace the potential terms in Eqs. (2.6) to (2.9) of paper I by

$$B3:\ (c/\beta)^4(k_F\beta)^9v(\mathbf{q},\mathbf{m}-\mathbf{n}+\mathbf{q})v(\mathbf{q}-\mathbf{q}_1,\mathbf{m}-\mathbf{n}+\mathbf{q}+\mathbf{q}_1)\times[v(\mathbf{q}_1,\mathbf{m}-\mathbf{n}+\mathbf{q}_1)-\tfrac{1}{2}v(\mathbf{m}-\mathbf{n}+\mathbf{q}_1,\mathbf{q}_1)], \tag{2.12}$$

$$H3:\ (c/\beta)^4(k_F\beta)^9v(\mathbf{q},\mathbf{m}-\mathbf{n}+\mathbf{q})v(\mathbf{q}_1,\mathbf{m}-\mathbf{n}+\mathbf{q}_1)\times[v(\mathbf{q}-\mathbf{q}_1,\mathbf{m}-\mathbf{n}+\mathbf{q}+\mathbf{q}_1)-\tfrac{1}{2}v(\mathbf{m}-\mathbf{n}+\mathbf{q}+\mathbf{q}_1,\mathbf{q}-\mathbf{q}_1)], \tag{2.13}$$

$$R3:\ (c/\beta)^4(k_F\beta)^9\{[v(\mathbf{q},\mathbf{m}+\mathbf{q}-\mathbf{q}_1)-\tfrac{1}{2}v(\mathbf{m}+\mathbf{q}-\mathbf{q}_1,\mathbf{q})]\times[v(\mathbf{q},\mathbf{n}-\mathbf{q}_1)-\tfrac{1}{2}v(\mathbf{n}-\mathbf{q}_1,\mathbf{q})]\times[v(\mathbf{q},\mathbf{n}-\mathbf{m}-\mathbf{q})-\tfrac{1}{2}v(\mathbf{n}-\mathbf{m}-\mathbf{q},\mathbf{q})]-\tfrac{3}{8}v(\mathbf{m}+\mathbf{q}-\mathbf{q}_1,\mathbf{q})v(\mathbf{n}-\mathbf{q}_1,\mathbf{q})v(\mathbf{n}-\mathbf{m}-\mathbf{q},\mathbf{q})\}, \tag{2.14}$$

$$F3:\ (c/\beta)^4(k_F\beta)^9v(\mathbf{q},\mathbf{m}-\mathbf{n}+\mathbf{q})[v(\mathbf{q},\mathbf{m}-\mathbf{n}+\mathbf{q})-\tfrac{1}{2}v(\mathbf{m}-\mathbf{n}+\mathbf{q},\mathbf{q})][2v(0,\mathbf{m}+\mathbf{q}_1)-v(\mathbf{m}+\mathbf{q}_1,0)-2v(0,\mathbf{q}+\mathbf{m}+\mathbf{q}_1)+v(\mathbf{q}+\mathbf{m}+\mathbf{q}_1,0)]. \tag{2.15}$$

For fourth order we may again simply replace the potential terms in Eq. (2.10) to (2.20) of paper I. For class I, the new term is [note that the factor $(k_Fc)^{-3}$ in (2.10) and (2.11) of paper I should have read $(k_Fc)^{-6}$]

$$(c/\beta)^6(k_F\beta)^{12}v(\mathbf{q},\mathbf{m}-\mathbf{n}+\mathbf{q})v(\mathbf{x}_2,\mathbf{y}_2)v(\mathbf{x}_3,\mathbf{y}_3)\times[v(\mathbf{x}_4,\mathbf{x}_5)-\tfrac{1}{2}v(\mathbf{x}_5,\mathbf{x}_4)]. \tag{2.16}$$

The $\mathbf{x}_i$ are tabulated in paper I and the y_i are given in Table I of this paper. For class IA the new potential

TABLE I. Arguments of the potentials.

Diagram	$\mathbf{y}_2$	$\mathbf{y}_3$
I.1	$\mathbf{m}-\mathbf{n}+\mathbf{q}+\mathbf{q}_1$	$\mathbf{m}-\mathbf{n}+\mathbf{q}_1+\mathbf{q}_2$
I.2	$\mathbf{m}-\mathbf{n}+\mathbf{q}+\mathbf{q}_1$	$\mathbf{m}-\mathbf{n}+\mathbf{q}_1+\mathbf{q}_2$
I.3+4	$\mathbf{m}-\mathbf{n}+\mathbf{q}_1+\mathbf{q}_2$	$\mathbf{m}-\mathbf{n}+\mathbf{q}+\mathbf{q}_2$
I.6	$\mathbf{m}-\mathbf{n}+\mathbf{q}_2+\mathbf{q}$	$\mathbf{m}-\mathbf{n}+\mathbf{q}_1+\mathbf{q}_2$
II.1	$\mathbf{m}-\mathbf{n}+\mathbf{q}$	
II.4	$\mathbf{m}-\mathbf{n}+\mathbf{q}$	
II.5	$\mathbf{m}-\mathbf{n}+\mathbf{q}$	
II.6	$\mathbf{q}+\mathbf{q}_2-\mathbf{m}-\mathbf{q}_1$	
II.7	$\mathbf{m}-\mathbf{n}+\mathbf{q}$	
II.9	$\mathbf{m}-\mathbf{n}+\mathbf{q}$	
II.10	$\mathbf{q}_2-\mathbf{m}$	
II.11	$\mathbf{m}-\mathbf{n}+\mathbf{q}$	

[3] J. Goldstone, Proc. Roy. Soc. (London) **A239**, 267 (1957).
[4] A. M. Green, Nucl. Phys. **33**, 218 (1962); Phys. Letters **1**, 136 (1962).
[5] J. Da Providenca, Nucl. Phys. **40**, 321 (1963).

term is

$$(c/\beta)^6(k_F\beta)^{12}$$
$$\times\{[v(\mathbf{q},\mathbf{x}_2)-\tfrac{1}{2}v(\mathbf{x}_2,\mathbf{q})][v(\mathbf{q},\mathbf{x}_3)-\tfrac{1}{2}v(\mathbf{x}_3,\mathbf{q})]$$
$$\times[v(\mathbf{q},\mathbf{x}_4)-\tfrac{1}{2}v(\mathbf{x}_4,\mathbf{q})][v(\mathbf{q},\mathbf{x}_5)-\tfrac{1}{2}v(\mathbf{x}_5,\mathbf{q})]$$
$$+\tfrac{3}{16}v(\mathbf{x}_2,\mathbf{q})v(\mathbf{x}_3,\mathbf{q})v(\mathbf{x}_4,\mathbf{q})v(\mathbf{x}_5,\mathbf{q})\}. \quad (2.17)$$

For class II the new potential term is

$$(c/\beta)^6(k_F\beta)^{12}\{v(\mathbf{x}_1,\mathbf{y}_2)[v(\mathbf{x}_2,\mathbf{x}_3)-\tfrac{1}{2}v(\mathbf{x}_3,\mathbf{x}_2)]$$
$$\times[v(\mathbf{x}_4,\mathbf{x}_5)-\tfrac{1}{2}v(\mathbf{x}_5,\mathbf{x}_4)][v(\mathbf{x}_4,\mathbf{x}_6)-\tfrac{1}{2}v(\mathbf{x}_6,\mathbf{x}_4)]$$
$$-\tfrac{3}{8}v(\mathbf{x}_1,\mathbf{y}_2)v(\mathbf{x}_3,\mathbf{x}_2)v(\mathbf{x}_5,\mathbf{x}_4)v(\mathbf{x}_6,\mathbf{x}_4)\}. \quad (2.18)$$

In order to write out the new potential term for class IIA it is convenient to define

$$\begin{aligned} v_1&=v(\mathbf{x}_1,\mathbf{x}_2), \quad v_2=v(\mathbf{x}_2,\mathbf{x}_1)\\ v_3&=v(\mathbf{x}_3,\mathbf{x}_4), \quad v_4=v(\mathbf{x}_4,\mathbf{x}_3)\\ v_5&=v(\mathbf{x}_1,\mathbf{x}_5), \quad v_6=v(\mathbf{x}_5,\mathbf{x}_1)\\ v_7&=v(\mathbf{x}_3,\mathbf{x}_6), \quad v_8=v(\mathbf{x}_6,\mathbf{x}_3). \end{aligned} \quad (2.19)$$

Then the new potential term is

$$(c/\beta)^6(k_F\beta)^{12}\{v_1v_3v_5v_7+v_1v_4v_5v_8+v_2v_3v_6v_7$$
$$-\tfrac{1}{2}(v_1v_3v_5v_8+v_1v_3v_6v_7+v_1v_4v_5v_7+v_1v_4v_6v_8$$
$$+v_2v_3v_5v_7+v_2v_3v_6v_8+v_2v_4v_5v_8+v_2v_4v_6v_7)$$
$$+\tfrac{1}{4}(v_1v_3v_6v_8+v_1v_4v_6v_7+v_2v_3v_5v_8$$
$$+v_2v_4v_5v_7+v_2v_4v_6v_8)\}. \quad (2.20)$$

For class III the new potential term is

$$(c/\beta)^6(k_F\beta)^{12}v(\mathbf{q},\mathbf{m}-\mathbf{n}+\mathbf{q})$$
$$\times[v(\mathbf{q},\mathbf{m}-\mathbf{n}+\mathbf{q})-\tfrac{1}{2}v(\mathbf{m}-\mathbf{n}+\mathbf{q},\mathbf{q})]$$
$$\times v(\mathbf{x}_2\mathbf{x}_3)[v(\mathbf{x}_2,\mathbf{x}_3)-\tfrac{1}{2}v(\mathbf{x}_3,\mathbf{x}_2)]. \quad (2.21)$$

For diagram IV.1 the new potential term is

$$(c/\beta)^6(k_F\beta)^{12}v(\mathbf{q},\mathbf{m}-\mathbf{n}+\mathbf{q})$$
$$\times[v(\mathbf{q},\mathbf{m}-\mathbf{n}+\mathbf{q})-\tfrac{1}{2}v(\mathbf{m}-\mathbf{n}+\mathbf{q},\mathbf{q})]$$
$$\times[-2v(0,\mathbf{m}+\mathbf{q}+\mathbf{m}_1)+v(\mathbf{m}+\mathbf{q}+\mathbf{m}_1,0)$$
$$-2v(0,\mathbf{n}-\mathbf{q}+\mathbf{m}_1)+v(\mathbf{n}-\mathbf{q}+\mathbf{m}_1,0)+2v(0,\mathbf{m}+\mathbf{m}_1)$$
$$-v(\mathbf{m}+\mathbf{m}_1,0)+2v(0,\mathbf{n}+\mathbf{m}_1)-v(\mathbf{n}+\mathbf{m}_1,0)]$$
$$\times[-2v(0,\mathbf{m}+\mathbf{q}+\mathbf{m}_2)+v(\mathbf{m}+\mathbf{q}+\mathbf{m}_2,0)$$
$$-2v(0,\mathbf{n}-\mathbf{q}+\mathbf{m}_2)+v(\mathbf{n}-\mathbf{q}+\mathbf{m}_2,0)+2v(0,\mathbf{m}+\mathbf{m}_2)$$
$$-v(\mathbf{m}+\mathbf{m}_2,0)+2v(0,\mathbf{n}+\mathbf{m}_2)-v(\mathbf{n}+\mathbf{m}_2,0)] \quad (2.22)$$

and for diagram IV.2 it is

$$(c/\beta)^6(k_F\beta)^{12}v(\mathbf{q},\mathbf{m}-\mathbf{n}+\mathbf{q})v(\mathbf{q}-\mathbf{q}_1,\mathbf{m}-\mathbf{n}+\mathbf{q}+\mathbf{q}_1)$$
$$\times[v(\mathbf{q}_1,\mathbf{m}-\mathbf{n}+\mathbf{q}_1)-\tfrac{1}{2}v(\mathbf{m}-\mathbf{n}+\mathbf{q}_1,\mathbf{q}_1)]$$
$$\times[-2v(0,\mathbf{m}+\mathbf{q}+\mathbf{m}_1)+v(\mathbf{m}+\mathbf{q}+\mathbf{m}_1,0)$$
$$+2v(0,\mathbf{m}+\mathbf{m}_1)-v(\mathbf{m}+\mathbf{m}_1,0)]. \quad (2.23)$$

For diagram IV.4 it is

$$(c/\beta)^6(k_F\beta)^{12}\{[v(\mathbf{q},\mathbf{m}-\mathbf{n}+\mathbf{q})-\tfrac{1}{2}v(\mathbf{m}-\mathbf{n}+\mathbf{q},\mathbf{q})]$$
$$\times[v(\mathbf{q},\mathbf{n}-\mathbf{q}_1)-\tfrac{1}{2}v(\mathbf{n}-\mathbf{q}_1,\mathbf{q})]$$
$$\times[v(\mathbf{q},\mathbf{m}+\mathbf{q}-\mathbf{q}_1)-\tfrac{1}{2}v(\mathbf{m}+\mathbf{q}-\mathbf{q}_1,\mathbf{q})]$$
$$-\tfrac{3}{8}v(\mathbf{m}-\mathbf{n}+\mathbf{q},\mathbf{q})v(\mathbf{n}-\mathbf{q}_1,\mathbf{q})v(\mathbf{m}+\mathbf{q}-\mathbf{q}_1,\mathbf{q})\}$$
$$\times[-2v(0,\mathbf{m}+\mathbf{q}+\mathbf{m}_1)+v(\mathbf{m}+\mathbf{q}+\mathbf{m}_1,0)$$
$$-2v(0,\mathbf{n}-\mathbf{q}+\mathbf{m}_1)+v(\mathbf{n}-\mathbf{q}+\mathbf{m}_1,0)+2v(0,\mathbf{m}+\mathbf{m}_1)$$
$$-v(\mathbf{m}+\mathbf{m}_1,0)+2v(0,\mathbf{n}+\mathbf{m}_1)-v(\mathbf{n}+\mathbf{m}_1,0)] \quad (2.24)$$

and for diagram IV.6 it is

$$(c/\beta)^6(k_F\beta)^{12}v(\mathbf{q},\mathbf{m}-\mathbf{n}+\mathbf{q})v(\mathbf{q}-\mathbf{q}_1,\mathbf{m}-\mathbf{n}+\mathbf{q}+\mathbf{q}_1)$$
$$\times[v(\mathbf{q}_1,\mathbf{m}-\mathbf{n}+\mathbf{q}_1)-\tfrac{1}{2}v(\mathbf{m}-\mathbf{n}+\mathbf{q}_1,\mathbf{q}_1)]$$
$$\times[-2v(0,\mathbf{m}+\mathbf{q}+\mathbf{m}_1)+v(\mathbf{m}+\mathbf{q}+\mathbf{m}_1,0)$$
$$+2v(0,\mathbf{m}+\mathbf{m}_1)-v(\mathbf{m}_1+\mathbf{m}_1,0)]. \quad (2.25)$$

We have now written out all the modifications made to the integrals given in paper I. The explicit integrals and diagrams are listed and drawn therein. We have evaluated them by the same Monte Carlo method as used before, using 1×10^5 to 2×10^6 Monte Carlo repetitions. As a minor variant we have found it more efficient to let the angle (rather than the cosine of the angle) between $\mathbf{q}$ and $\mathbf{q}_1$ be uniformly distributed in diagrams B3, I.1, II.1, II.5 and II.6 (also the angle between $\mathbf{q}_1$ and $\mathbf{q}_2$ in I.1). This change tends to emphasize the parallel and antiparallel momenta.

We shall now tabulate (Table II) our best values for each diagram along with an estimate of the standard deviation for a selection of densities. As the calculations are fairly lengthy, we have not attempted to get accurate values of the smaller diagrams. The diagrams which are included in the Brueckner approximation[6] are B1, B2, B3, F3, I.1, III.1, III.7+8, IV.1, IV.2, and IV.3.

III. COMPARISON OF THE RESULTS WITH THE LADDER AND BRUECKNER APPROXIMATIONS

We shall sum the perturbation series coefficients derived in the previous section by the Padé approximant method.[7] It is doubtless true that the perturbation series for the many-fermion energy, as well as for the ladder and Brueckner approximations to it are asymptotic series for our potential, as has been shown for the soft, repulsive, square-well potential.[8] However, it is also probably true for this potential, at least for low enough density (and, we feel, for all densities for this potential), that there is a unique, regular function of the strength V for positive real V, $0<V<1$.

We shall now determine the nature of the ladder approximation series. Let v be the two-body potential

[6] K. A. Brueckner, *The Many-Body Problem*, edited by C. deWitt (John Wiley & Sons, Inc., New York, 1959), pp. 65 ff.

[7] G. A. Baker, Jr., and J. L. Gammel, J. Math. Anal. Appl. **2**, 21 (1961); G. A. Baker, Jr., J. L. Gammel, and J. G. Wills, J. Math. Anal. Appl. **2**, 405 (1961); H. S. Wall, *Continued Fractions* (D. Van Nostrand Company, Inc., Princeton, New Jersey), Chap. XX; and Ref. 10 of paper I.

[8] G. A. Baker, Jr., Phys. Rev. **131**, 1869 (1963).

operator, and $1/b_i=P/(H_0-E_i)$, where H_0 is the two-body kinetic energy operator, E_i the unperturbed energy of the relevant two-body state, and P a projection operator which is zero for states in the Fermi sea and unity otherwise. The energy shift is then, in ladder approximation,

$$\Delta E=\sum_i\left\langle\psi_i\left|v\lambda-v\frac{1}{b_i}v\lambda^2+v\frac{1}{b_i}v\frac{1}{b_i}v\lambda^3-v\frac{1}{b_i}v\frac{1}{b_i}v\frac{1}{b_i}v\lambda^4+\cdots\right|\psi_i\right\rangle, \tag{3.1}$$

where the sum on i is over the Fermi sea and λ is regarded as an expansion parameter. The operator v is not positive definite as it was for the soft, repulsive, square-well case discussed in paper I; however, we may proceed as follows. Equation (3.1) may be rewritten as

$$\begin{aligned}\Delta E&=[\sum_i\langle\psi_i|v|\psi_i\rangle]\lambda-\lambda^2\left[\sum_i\left\langle\varphi_i\left|1-\left(\frac{1}{b_i^{1/2}}v\frac{1}{b_i^{1/2}}\right)\lambda+\left(\frac{1}{b_i^{1/2}}v\frac{1}{b_i^{1/2}}\right)^2\lambda^2-\left(\frac{1}{b_i^{1/2}}v\frac{1}{b_i^{1/2}}\right)^3\lambda^3+\cdots\right|\varphi_i\right\rangle\right]\\&=[\sum_i\langle\psi_i|v|\psi_i\rangle]\lambda-\lambda^2[\sum_i\langle\varphi_i|1-V_i\lambda+V_i^2\lambda^2-V_i^3\lambda^3+\cdots|\varphi_i\rangle],\end{aligned} \tag{3.2}$$

where $\varphi_i=(1/b_i^{1/2})v\psi_i$. Now the operator V_i is Hermitian because v is Hermitian and, in momentum

TABLE II. Monte Carlo calculations.

Diagram	$k_F\beta=0.5$ Value	Deviation	$k_F\beta=1.0$ Value	Deviation
B1[a]	3.4043171×10^{-2}		3.5338219×10^{-1}	
B2[a]	-3.772×10^{-2}	8.3×10^{-5}	-2.206×10^{-1}	4.0×10^{-4}
B3[a]	8.665×10^{-2}	2.1×10^{-4}	4.418×10^{-1}	2.1×10^{-3}
H3	1.20×10^{-3}	1.2×10^{-5}	2.01×10^{-2}	2.3×10^{-4}
R3	-5.84×10^{-3}	2.3×10^{-5}	-8.27×10^{-2}	5.6×10^{-4}
F3[a]	1.81×10^{-3}	1.4×10^{-5}	6.91×10^{-2}	6.0×10^{-4}
Σ3	8.382×10^{-2}	2.1×10^{-4}	4.483×10^{-1}	2.3×10^{-3}
Br 3	8.846×10^{-2}	2.1×10^{-4}	5.109×10^{-1}	2.2×10^{-3}
I.1[a]	-2.29×10^{-1}	1.4×10^{-3}	-9.04×10^{-1}	1.5×10^{-2}
I.2	-2.10×10^{-3}	2.3×10^{-5}	-3.55×10^{-2}	5.8×10^{-4}
I.3+4	-1.57×10^{-3}	1.9×10^{-5}	-1.92×10^{-2}	4.0×10^{-4}
I.5[b]	-2.10×10^{-3}	2.3×10^{-5}	-3.55×10^{-2}	5.8×10^{-4}
I.6	-1.18×10^{-4}	2.4×10^{-6}	-4.75×10^{-3}	1.3×10^{-4}
IA.1	-5.59×10^{-4}	7.4×10^{-6}	-1.80×10^{-2}	3.2×10^{-4}
IA.2	-2.10×10^{-4}	1.9×10^{-6}	-4.68×10^{-3}	8.5×10^{-5}
IA.3	-4.97×10^{-4}	6.2×10^{-6}	-1.54×10^{-2}	5.4×10^{-4}
II.1	1.07×10^{-2}	1.4×10^{-4}	1.58×10^{-1}	3.7×10^{-3}
II.2[b]	1.07×10^{-2}	1.4×10^{-4}	1.58×10^{-1}	3.7×10^{-3}
II.3	$+2.88\times10^{-4}$	3.7×10^{-6}	1.036×10^{-2}	2.3×10^{-4}
II.4[b]	$+2.88\times10^{-4}$	3.7×10^{-6}	1.036×10^{-2}	2.3×10^{-4}
II.5	3.37×10^{-3}	5.6×10^{-5}	4.05×10^{-2}	1.4×10^{-3}
II.6	5.25×10^{-3}	1.4×10^{-4}	5.81×10^{-2}	2.5×10^{-3}
II.7	-2.78×10^{-4}	2.4×10^{-6}	-6.63×10^{-3}	1.4×10^{-4}
II.8	-3.23×10^{-4}	2.8×10^{-6}	-7.27×10^{-3}	1.4×10^{-4}
II.9	$+1.46\times10^{-4}$	2.8×10^{-6}	2.84×10^{-3}	1.5×10^{-4}
II.10	6.48×10^{-5}	1.7×10^{-6}	2.42×10^{-3}	1.2×10^{-4}
II.11[b]	-3.23×10^{-4}	2.8×10^{-6}	-7.27×10^{-3}	1.4×10^{-4}
II.12[b]	-2.78×10^{-4}	2.4×10^{-6}	-6.63×10^{-3}	1.4×10^{-4}
IIA.1	-3.59×10^{-3}	2.7×10^{-5}	-5.58×10^{-2}	9.0×10^{-4}
IIA.2	5.85×10^{-4}	8.0×10^{-6}	2.35×10^{-2}	5.2×10^{-4}
IIA.3	-1.046×10^{-4}	1.7×10^{-6}	-4.98×10^{-3}	1.5×10^{-4}
IIA.4[b]	5.85×10^{-4}	8.0×10^{-6}	2.35×10^{-2}	5.2×10^{-4}
IIA.5	4.02×10^{-4}	4.0×10^{-6}	9.82×10^{-3}	3.4×10^{-4}
IIA.6	3.88×10^{-4}	4.4×10^{-6}	8.79×10^{-3}	3.0×10^{-4}
III.1[a]	-7.75×10^{-3}	1.0×10^{-4}	-1.30×10^{-1}	2.6×10^{-3}
III.2	-5.20×10^{-4}	8.1×10^{-6}	-1.82×10^{-2}	5.4×10^{-4}
III.7+8[a]	8.99×10^{-3}	9.1×10^{-5}	1.23×10^{-1}	2.2×10^{-3}
III.9+10	6.76×10^{-4}	1.1×10^{-5}	1.88×10^{-2}	4.9×10^{-4}
IV.1[a]	-7.44×10^{-5}	3.6×10^{-7}	-2.15×10^{-2}	8.8×10^{-5}
IV.2[a]	-3.72×10^{-3}	1.1×10^{-4}	-1.31×10^{-1}	3.2×10^{-3}
IV.3[a,b]	-3.72×10^{-3}	1.1×10^{-4}	-1.31×10^{-1}	3.2×10^{-3}
IV.4	2.69×10^{-4}	9.6×10^{-7}	2.66×10^{-2}	2.1×10^{-4}
IV.5[b]	2.69×10^{-4}	9.6×10^{-7}	2.66×10^{-2}	2.1×10^{-4}
IV.6	-5.58×10^{-5}	2.8×10^{-6}	-6.45×10^{-3}	4.9×10^{-4}
IV.7[b]	-5.58×10^{-5}	2.8×10^{-6}	-6.45×10^{-3}	4.9×10^{-4}
Σ4	-2.14×10^{-1}	1.5×10^{-3}	-8.68×10^{-1}	1.9×10^{-2}
Br 4	-2.36×10^{-1}	1.4×10^{-3}	-1.195×10^{0}	1.7×10^{-2}

TABLE II (*continued*)

Diagram	$k_F\beta=1.5$ Value	Deviation	$k_F\beta=2.0$ Value	Deviation
B1[a]	1.5966883×10^{0}		5.0158397×10^{0}	
B2[a]	-6.639×10^{-1}	1.4×10^{-3}	-1.661×10^{0}	5.0×10^{-3}
B3[a]	1.054×10^{0}	1.0×10^{-2}	1.988×10^{0}	4.0×10^{-2}
H3	8.71×10^{-2}	1.6×10^{-3}	2.28×10^{-1}	7.2×10^{-3}
R3	-2.96×10^{-1}	5.3×10^{-3}	-6.46×10^{-1}	1.3×10^{-2}
F3[a]	6.37×10^{-1}	4.5×10^{-3}	3.59×10^{0}	2.6×10^{-2}
$\Sigma3$	1.482×10^{0}	1.2×10^{-2}	5.16×10^{0}	5.0×10^{-2}
Br 3	1.691×10^{0}	1.1×10^{-2}	5.58×10^{0}	4.8×10^{-2}
I.1[a]	-1.77×10^{0}	1.1×10^{-1}	-3.10×10^{0}	5.3×10^{-1}
I.2	-1.52×10^{-1}	4.9×10^{-3}	-3.85×10^{-1}	2.5×10^{-2}
I.3+4	-6.48×10^{-2}	3.3×10^{-3}	-1.43×10^{-1}	1.5×10^{-2}
I.5[b]	-1.52×10^{-1}	4.9×10^{-3}	-3.85×10^{-1}	2.5×10^{-2}
I.6	-3.19×10^{-2}	1.4×10^{-3}	-1.06×10^{-1}	7.5×10^{-3}
IA.1	-1.096×10^{-1}	2.8×10^{-3}	-3.96×10^{-1}	2.4×10^{-2}
IA.2	-2.26×10^{-2}	1.1×10^{-3}	-8.12×10^{-2}	9.3×10^{-3}
IA.3	-9.24×10^{-2}	6.3×10^{-3}	-3.60×10^{-1}	7.7×10^{-2}
II.1	5.93×10^{-1}	3.2×10^{-2}	1.45×10^{0}	1.0×10^{-1}
II.2[b]	5.93×10^{-1}	3.2×10^{-2}	1.45×10^{0}	1.0×10^{-1}
II.3	6.37×10^{-2}	3.0×10^{-3}	2.12×10^{-1}	1.9×10^{-2}
II.4[b]	6.37×10^{-2}	3.0×10^{-3}	2.12×10^{-1}	1.9×10^{-2}
II.5	1.26×10^{-1}	8.3×10^{-3}	2.11×10^{-1}	4.0×10^{-2}
II.6	1.57×10^{-1}	1.4×10^{-2}	2.03×10^{-1}	4.9×10^{-2}
II.7	-2.75×10^{-2}	1.7×10^{-3}	-6.2×10^{-2}	1.0×10^{-2}
II.8	-3.27×10^{-2}	1.9×10^{-3}	-7.7×10^{-2}	1.2×10^{-2}
II.9	4.93×10^{-3}	1.9×10^{-3}	-2.8×10^{-3}	7.8×10^{-3}
II.10	1.49×10^{-2}	1.3×10^{-3}	4.50×10^{-2}	7.1×10^{-3}
II.11[b]	-3.27×10^{-2}	1.9×10^{-3}	-7.7×10^{-2}	1.2×10^{-2}
II.12[b]	-2.75×10^{-2}	1.7×10^{-3}	-6.2×10^{-2}	1.0×10^{-2}
IIA.1	-2.61×10^{-1}	9.4×10^{-3}	-9.74×10^{-1}	7.0×10^{-2}
IIA.2	1.88×10^{-1}	6.9×10^{-3}	8.59×10^{-1}	5.7×10^{-2}
IIA.3	-3.63×10^{-2}	2.3×10^{-3}	-1.39×10^{-1}	1.7×10^{-2}
IIA.4[b]	1.88×10^{-1}	6.9×10^{-3}	8.59×10^{-1}	5.7×10^{-2}
IIA.5	5.41×10^{-2}	5.3×10^{-3}	1.77×10^{-1}	3.6×10^{-2}
IIA.6	4.08×10^{-2}	4.0×10^{-3}	1.18×10^{-1}	2.6×10^{-2}
III.1[a]	-7.64×10^{-1}	2.9×10^{-2}	-3.30×10^{0}	2.2×10^{-1}
III.2	-1.23×10^{-1}	7.1×10^{-3}	-5.03×10^{-1}	4.6×10^{-2}
III.7+8[a]	5.61×10^{-1}	2.6×10^{-2}	1.88×10^{0}	2.7×10^{-1}
III.9+10	1.06×10^{-1}	6.0×10^{-3}	3.99×10^{-1}	4.0×10^{-2}
IV.1[a]	-6.11×10^{-1}	3.6×10^{-3}	-7.68×10^{0}	7.8×10^{-2}
IV.2[a,b]	-1.02×10^{0}	3.4×10^{-2}	-4.51×10^{0}	2.7×10^{-1}
IV.3[a]	-1.02×10^{0}	3.4×10^{-2}	-4.51×10^{0}	2.7×10^{-1}
IV.4	2.94×10^{-1}	8.0×10^{-3}	1.24×10^{0}	1.2×10^{-1}
IV.5[b]	2.94×10^{-1}	8.0×10^{-3}	1.24×10^{0}	1.2×10^{-1}
IV.6	-8.50×10^{-2}	7.6×10^{-3}	-5.13×10^{-1}	5.7×10^{-2}
IV.7[b]	-8.50×10^{-2}	7.6×10^{-3}	-5.13×10^{-1}	5.7×10^{-2}
$\Sigma4$	-3.18×10^{0}	1.5×10^{-1}	-1.73×10^{1}	9.2×10^{-1}
Br 4	-4.62×10^{0}	1.4×10^{-1}	-2.12×10^{1}	8.4×10^{-1}

[a] Included in the Brueckner approximation.
[b] Identical with a previous diagram (but must be added to find the total fourth-order coefficient).

representation, $1/b_i$ is non-negative definite so that $1/b_i^{1/2}$ is real and non-negative definite. The eigenvalues of V_i are greater than -1. To see this result, we first note that, due to the P in $1/b_i^{1/2}$, the φ_i must be expandable in terms of

$$\exp[i(\mathbf{q}+\mathbf{m})\cdot\mathbf{r}_1+i(\mathbf{n}-\mathbf{q})\cdot\mathbf{r}_2], \quad |\mathbf{q}+\mathbf{m}|>k_F, \quad |\mathbf{n}-\mathbf{q}|>k_F. \tag{3.3}$$

The eigenvalue equation is

$$V_i\varphi=\Gamma\varphi, \tag{3.4}$$

where we seek the smallest Γ. The value of E_i in V_i is

$$2E_i=m^2+n^2=\tfrac{1}{2}(\mathbf{m}+\mathbf{n})^2+\tfrac{1}{2}(\mathbf{m}-\mathbf{n})^2. \tag{3.5}$$

Substituting

$$\varphi=(H_0-E_i)^{1/2}\omega, \tag{3.6}$$

where ω must also have the form (3.3), Eq. (3.4) may be written as

$$v\omega=\Gamma(H_0-E_i)\omega. \tag{3.7}$$

If we let H_r be the relative Hamiltonian and r the separation distance $|\mathbf{r}_1-\mathbf{r}_2|$, then separating off the center-of-mass motion of the pair, Eq. (3.7) becomes

$$[H_r-(1/\Gamma)v]\omega=\tfrac{1}{4}(\mathbf{m}-\mathbf{n})^2\omega. \tag{3.8}$$

For simplicity, and without loss of generality, we select $\mathbf{m}=\mathbf{n}=0$. The eigenvalue problem now becomes

$$[H_r-(1/\Gamma)v]\omega\equiv\mathfrak{M}_\Gamma\omega=0, \quad q>k_F. \tag{3.9}$$

Now because of the term $-\Lambda/r^2$ in H_r, the operator $\mathfrak{M}_\Gamma$ is non-negative for $\Gamma<-1$ [see Eqs. (2.1) and (2.5)]. In fact, because of the restriction $q>k_F$, the smallest eigenvalue of $\mathfrak{M}_\Gamma$ is strictly positive for $\Gamma<-1$. Thus, V_i has no eigenvalues less than -1. Minus one is also the greatest lower bound for the eigenvalues of V_i. This result is not necessary here, but can be seen from the results given by Morse and Feshbach.[9]

If we now expand the φ_i of (3.2) in a complete, orthonormal set of wave functions ω_{ik} which are eigenfunctions of V_i in the allowed subspace, Eq. (3.2) becomes

$$\Delta E=[\sum_i\langle\psi_i|v|\psi_i\rangle]\lambda-\lambda^2\{\sum_i[\sum_k(1-V_{ik}\lambda+V_{ik}{}^3\lambda^2 - V_{ik}{}^3\lambda^3+\cdots)|a_{ik}|^2]\}. \quad (3.10)$$

Since $|a_{ik}|^2\geq 0$, a id it is easily demonstrated that

$$\sum_i\left\langle\psi_i\left|\frac{1}{v-v_{b_i}}\right|\psi_i\right\rangle=\sum_{i,k}|a_{ik}|^2 \quad (3.11)$$

is finite, and if we denote by $-(-1)^pc_p$ the coefficient of λ^{p+2} in (3.10), then there exists a nondecreasing function $\varphi(u)$ such that

$$c_p=\int_{-1}^{\infty}u^p d\varphi(u), \quad p=0, 1, 2, \cdots. \quad (3.12)$$

The function φ will take on infinitely many values if and only if there are infinitely many eigenvalues involved. Thus we may formally sum the ladder series as

$$\Delta E=c_{-1}\lambda-\lambda\int_{-1}^{\infty}\frac{\lambda d\varphi(u)}{1+u\lambda}. \quad (3.13)$$

If we let

$$\eta=\lambda/(1-\lambda), \quad v=u+1, \quad \Phi(v)=\varphi(v-1), \quad (3.14)$$

then we may rewrite (3.13) as

$$c_{-1}-\frac{\Delta E[\eta/(1+\eta)]}{\eta/(1+\eta)}=\int_0^{\infty}\frac{\eta d\Phi(v)}{1+\eta v}. \quad (3.15)$$

The form on the right-hand side is necessary and sufficient for that function to be a series of Stieltjes.[10] As the coefficients only diverge like $p!$ we are dealing (Theorem 88.1)[10] with the case of a unique Φ. {An additional complication appears in the proof of this divergence rate for this potential; namely the potential [Eq. (2.5)] diverges like $q_{\text{exch}}{}^2$ when $q_{\text{exch}}\gg q$, rather than going to zero like q^{-2} as with the soft, repulsive square-well. As is apparent through fourth order from the results of the previous section, one can show that none of the perturbaton series diagrams diverge for infinite values of the internal momentum on this account and nothing extraordinary happens at infinity. Consequently the arguments bounding the rate of divergence of the series remain essentially as they were for the square-well potential.[8]} Using (3.15), the fact that

$$\{\Delta E[\eta/(1+\eta)]-c_{-1}[\eta/(1+\eta)]+c_0[\eta/(1+\eta)]^2\}\times(1+\eta)^2/\eta^2 \quad (3.16)$$

is also a series of Stieltjes, Wall's problem[10] (17.3), and some elementary properties of the Padé approximants,[7] we may prove

$$[n, n+1](\lambda)>\Delta E(\lambda)>[n, n+2](\lambda), \quad 0<\lambda<1 \quad (3.17)$$

for the energy shift in ladder approximation. We note that the $[n+1, n+1]$ lies between the bounds given in (3.17) and presumably is closer to the exact answer though not necessarily a lower bound as it was for the soft, repulsive, square-well potential.

We have plotted in Fig. 1 the [2,2] Padé approximants at $V=1.0$ (the two-body, hard-core equivalent) to the complete perturbation series, the ladder approximation, and the Brueckner approximation. We have divided by the first-order energy to provide an appropriate scale. Unity is, of course, a rigorous upper bound for the energy. We estimate from the rigorous upper and lower bounds for the ladder approximation, the internal consistency between the [1,2] and [1,3] Padé approximants for the other cases and the statistical error in the coefficients indicate that accuracy of the curves is about 3% near $k_F\beta=0$. The accuracy improves to about 1% near $k_F\beta=1.0$ and declines to around 2% near $k_F\beta=2.0$. We believe that, except near crossing points, the relative accuracy is sufficient to order correctly the various approximations.

The qualitative features are similar to those obtained for a soft, repulsive, square-well in paper I. At low density ($k_F\beta\leq 0.5$), the Brueckner approximation again lies above the ladder approximation while the complete perturbation series lies below the ladder approximation. At high densities ($k_F\beta>1.0$), the complete perturbation series lies above the Brueckner approximation which, in turn, lies above the ladder approximation. Here the flag (bubble) diagrams dominate the series for this potential and thus the Brueckner approximation is much more accurate than the ladder.

Quantitatively, the differences between the various curves is much smaller than for the repulsive square-well. Except at high density, where the ladder approximation falls decidedly below the others, the differences are relatively insignificant. The much smaller differences are probably due to this potential being much better suited to perturbative treatment than the hard-core potential.[11] By this statement we mean that when

[9] P. M. Morse and H. Feshbach, *Methods of Theoretical Physics* (McGraw-Hill Book Company, Inc., New York, 1953), p. 1666.

[10] H. S. Wall, *Analytic Theory of Continued Fractions* (D. Van Nostrand Company, Inc., New York, 1948), Chap. XVII.

[11] The suggestion that this advantage might exist was first made, we believe, by R. E. Peierls, *Proceedings of the International Conference on Nuclear Structure, Kingston* (University of Toronto Press, Toronto, 1960), p. 7.

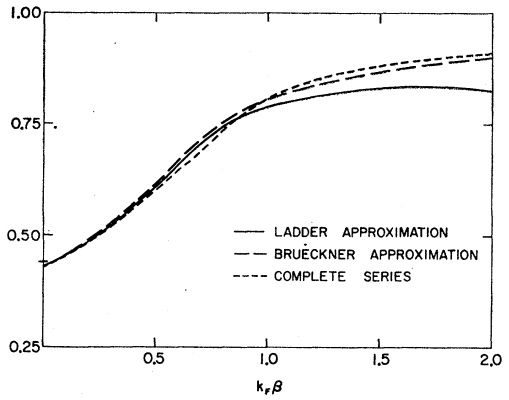

FIG. 1. Sum of complete perturbation series, ladder approximation series, and Brueckner approximation series as given by the [2,2] Padé approximant in units of the first-order coefficient. The tick mark on the left border is the exact zero density value.

calculating by series expansion a function near an argument of unity, the omission of sequences of terms starting in third and higher orders is apparently less important than doing so in the calculation of the value of a function near an argument of infinity.

The point at $k_F\beta=0.0$ was obtained as follows. For zero densities, as is well known, all the curves tend to the zero-energy scattering length for the potential in question. We may compute the scattering length for our potential by solving the differential equation

$$(1+Vse^{-r})u''-Vse^{-r}u' +0.25V[se^{-r}-0.25s^2e^{-2r}(1+se^{-r})^{-1}]u=0. \quad (3.18)$$

We have solved this numerically and differenced the resultant scattering lengths as a function of V. We find that the energy is given by

$$\lim_{k_F\to 0}[E/(k_F\beta)^3]=0.242194V-0.4357V^2 +1.119V^3-3.312V^4+\cdots. \quad (3.19)$$

The Padé approximants are then computed from these coefficients.

In order to investigate the accuracy of the usual numerical solution procedures for the ladder and Brueckner approximations, we have used the method described in paper I, to which the reader is referred for more details, except it was necessary to modify some of the equations for the velocity-dependent force. Instead of I(5.7) we have for the Green's function (actually r^2VG)

$$\mathbf{G}_{kl}(r,r')=\frac{\pi}{2}Vse^{-r}\begin{cases}[l/(2l+1)](r/r')^{l+1} & r<r'\\ -(4l+2)^{-1} & r=r'\\ -[(l+1)/(2l+1)](r'/r)^{l} & r>r'\end{cases}$$
$$+se^{-r}Vr^2\int_0^\infty k''dk''\left[\frac{(k'')^2F(\bar{p},k'',k)}{2[E(k'')-\Delta(k)]}-1\right]j_l(k''r')\left[k''j_l(k''r)+\frac{l}{2l+1}j_{l-1}(k''r)-\frac{l+1}{2l+1}j_{l+1}(k''r)\right]$$
$$-r^2V\left\{\frac{1}{4}se^{-4}\left(1-\frac{4}{r}-\frac{\frac{1}{4}se^{-r}}{1+se^{-r}}\right)+l(l+1)\left(\frac{1+se^{-r}}{r^2}-\left[r+2\ln\left(\frac{1+(1+se^{-r})^{1/2}}{2}\right)\right]^{-2}\right)\right\}$$
$$\times\int_0^\infty k''^2dk''\frac{j_l(k''r)j_l(k''r')}{2[E(k'')-\Delta(k)]}F(\bar{p},k'',k). \quad (3.20)$$

The wave function ($X=r^2Vu$) satisfies the integral equation

$$(1+Vse^{-r})X_{kl}(r)+\frac{2}{\pi}\int_0^\infty \mathbf{G}_{kl}(r,r')X_{kl}(r')dr'$$
$$=-r^2V\left(se^{-r}\left[-k^2+\frac{1}{4}\left(1-\frac{4}{r}-\frac{\frac{1}{4}se^{-r}}{1+se^{-r}}\right)\right]+l(l+1)\left\{\frac{1+se^{-r}}{r^2}-\left[r+2\ln\left(\frac{1+(1+se^{-r})^{1/2}}{2}\right)\right]^{-2}\right\}\right)j_l(kr)$$
$$+r^2Vse^{-r}k\left[\frac{l}{2l+1}j_{l-1}(kr)-\frac{l+1}{2l+1}j_{l+1}(kr)\right] \quad (3.21)$$

instead of I(5.9), and the K matrices are given by

$$K_l(k)=\frac{2}{\pi}\int_0^\infty j_l(kr)X_{kl}(r)dr \quad (3.22)$$

instead of I(5.10). The rest of the equations and procedures remain unchanged except we now use a spacing of $\min[\frac{1}{2}\beta,1/(2k_F)]$ in the r meshes and carry them to 9β. (β is set to unity in the above equations.) A modified

trapezoidal rule based on the Euler-Maclaurin sum formula[12] is used on the discontinuous term in the Green's function to reduce the accumulation of integration errors due to its shape. Due to the cancellation between attractive and repulsive parts of this potential, it is essential to do a careful numerical job.

Since $V=1.0$ is a singular point, it should not be surprising to find that there is a very strong numerical cancellation on the left-hand side of (3.21) for this value. Consequently, the numerical results, except at low density, are not too accurate for $V=1.0$ and we have chosen to study $V=0.75$ and 0.875 instead. By comparison of the upper and lower bounds obtained by the Padé method with the results of the K-matrix solution for the ladder approximation, we conclude that the error increases from about one-tenth of a percent at zero density to of the order of 5% (low) at a density of two. We believe we have retained an adequate number of partial waves, namely one for $k_F\beta=10^{-4}$, three for $k_F\beta=0.5$, five for $k_F\beta=1.0$, and six for $k_F\beta=1.5$ and 2.0, which latter was the maximum number our computer program could conveniently handle.

We have calculated the Brueckner approximation for $V=0.75$. According to the Padé method, the shift from the ladder approximation for $k_F\beta=0.5$ and 1.0 is 0.9% and 2.2%, respectively. The K-matrix code gives shifts of 0.08% and 2.7% at these two points. The inconsistency of the shifts is no doubt due to Brueckner's treatment of off-energy shell effects as pointed out in paper I. For $k_F\beta=1.5$, the Padé method gives a shift of 3.7%; however, the K-matrix method fails to converge at this and higher densities. The failure of convergence at this point can perhaps be understood by reference to Table II. Between $k_F\beta=1.0$ and 1.5, the correction diagrams included in the Brueckner approximation become comparable in size to the ladder diagram. Thus it is not too surprising that an iterative type procedure of the sort needed to solve the K-matrix equation may fail with those relative magnitudes between the initial and correction terms. Referring to Fig. 1, we feel, although the Brueckner approximation is clearly superior to the ladder at high density for this potential, that, since the "as practiced" Brueckner approximation fails to converge there and is at least as inaccurate as the ladder approximation for lower density and is harder to compute, there is no practical advantage to the Brueckner approximation as practiced for the potentials we have investigated.

In order to give some idea of the differences which can arise in the solution of a many-body problem even though the two-body forces are equivalent for the simple two-body problem, we have plotted in Fig. 2 the ratio of the velocity-dependent force result to the hard core results of paper I in ladder approximation. That the ratio drops can be understood qualitatively

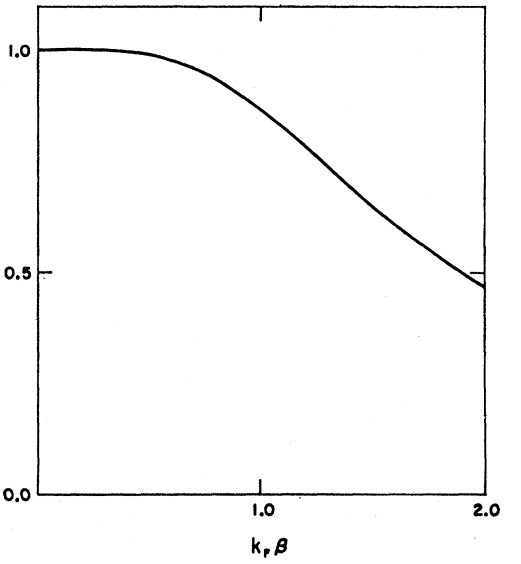

FIG. 2. Ratio of the hard-core simulating, velocity-dependent force energy shift to the hard-core force energy shift in the ladder approximation.

from the observation that the energy for the hard-core system goes to infinity at some jamming density, while for the velocity-dependent force the energy does not. Thus, even in ladder approximation, we would expect that the hard-core force would seem the stronger force.

IV. MOCK He^3

In this section we shall investigate the suggestion by Brueckner (paper I, Ref. 4) that the ring diagrams will not be as important corrections near equilibrium as the flag (bubble) diagrams are for potentials with long-range attractions and short-range repulsions. We select for our force

$$W(R)=\begin{cases}-Ae^{-R/\beta}[1-\frac{1}{4}se^{-R/\beta}]^{-2} & R\geq\beta\\ +\infty & R<\beta,\end{cases} \tag{4.1}$$

which is equivalent to the velocity-dependent force of Sec. II minus

$$V(r)=Ae^{-r/\beta} \tag{4.2}$$

with the Fourier transform

$$V(k)=8\pi A\beta^3[1+(k\beta)^2]^{-2}. \tag{4.3}$$

If we wish a potential similar to that between two He^4 atoms, according to Larsen,[13] we must pick a hard-core radius $\beta=2.1\times10^{-8}$ cm and a dimensionless strength slightly less than unity (0.96–0.997). If we assume the same strength of interaction for He^3, we get by solving Schrödinger's equation for the constant A, the dimensionless value

$$MA\beta^2/\hbar^2=2.5368, \tag{4.4}$$

which corresponds to unit strength for He^3. Using this

[12] See, for instance, P. Franklin, *A Treatise on Advanced Calculus* (John Wiley & Sons, Inc., New York, 1949), Sec. 322.

[13] S. Y. Larsen, Phys. Rev. **130**, 1426 (1963).

TABLE III. Monte Carlo calculations.

Diagram	$k_F\beta=0.75$ Value	Deviation	$k_F\beta=1.0$ Value	Deviation
B1	-4.573258×10^{-2}	...	-9.799826×10^{-2}	...
B2	-6.91×10^{-2}	5.8×10^{-4}	-1.67×10^{-1}	1.2×10^{-3}
B3	1.32×10^{-1}	1.8×10^{-3}	2.89×10^{-1}	5.3×10^{-3}
H3	1.23×10^{-3}	1.7×10^{-5}	6.71×10^{-3}	7.9×10^{-5}
R3	-5.44×10^{-3}	5.0×10^{-5}	-3.02×10^{-2}	2.1×10^{-4}
F3	4.85×10^{-3}	6.9×10^{-5}	3.82×10^{-2}	4.1×10^{-4}
$\Sigma3$	1.33×10^{-1}	1.8×10^{-3}	3.04×10^{-1}	5.3×10^{-3}
Br 3	1.37×10^{-1}	1.8×10^{-3}	3.27×10^{-1}	5.3×10^{-3}
	$k_F\beta=1.25$		$k_F\beta=1.50$	
B1	-1.2827432×10^{-1}	...	-5.62131×10^{-3}	...
B2	-3.337×10^{-1}	7.0×10^{-4}	-5.99×10^{-1}	3.3×10^{-3}
B3	5.24×10^{-1}	4.1×10^{-3}	7.81×10^{-1}	2.8×10^{-2}
H3	2.09×10^{-2}	2.6×10^{-4}	4.79×10^{-2}	7.4×10^{-4}
R3	-8.81×10^{-2}	6.8×10^{-4}	-1.84×10^{-1}	2.1×10^{-3}
F3	1.64×10^{-1}	1.6×10^{-3}	5.22×10^{-1}	5.6×10^{-3}
$\Sigma3$	6.21×10^{-1}	4.5×10^{-3}	1.167×10^{0}	2.9×10^{-2}
Br 3	6.88×10^{-1}	4.4×10^{-3}	1.303×10^{0}	2.9×10^{-2}

value of A one can calculate by the methods outlined below, that saturation occurs at roughly the right density ($2<k_F\beta<3$) but that the minimum implies substantially more binding energy than one observes experimentally (over four times as much). This lack of agreement is of no particular concern, because as we have pointed out in the previous section, at high densities the velocity-dependent force is much less repulsive than the hard core it simulates exactly at low density. Referring to Table II, we see that at high density the flag diagrams are dominant and the ring diagrams relatively small. This fact makes the region of the He^3 minimum a poor one to study cancellation of the ring-diagram correction to energy. We have therefore chosen A to be about one-half the value given in (4.4), i.e.,

$$MA\beta^2/\hbar^2=1.25. \tag{4.5}$$

The minimum of the energy turns out to be at about $k_F\beta=1.25$. We obtained this result by repeating the calculations described in Sec. II using a potential equal to that of (2.1) minus that of (4.2). We have computed through third order all the perturbation theory terms for $k_F\beta=0.75$, 1.00, 1.25, and 1.50. The Padé approximant method then enables us to select $k_F\beta=1.25$ as the value closest to saturation. As can be seen from a comparison of the results in Table III with those in Table II, while the magnitude of the ring diagram is reduced compared to its value for a purely repulsive force; so also, and by about the same factor, are all the other diagrams. This conclusion is reinforced and extended by the results for fourth order which we give in Table IV. We see, on the basis of these results, no reason to believe that being near saturation measurably improves the Brueckner approximation. In Table V we give, based on the [2,2] Padé approximant, the values of the ladder approximation, Brueckner approximation and complete theory for $k_F\beta=1.25$. The shift from the [1,2] approximants are 0.01 to 0.02. Thus we estimate the accuracy of these results to be 5% or better. The [1,2] and [1,3] Padé approximants again form rigorous upper and lower bounds. In order to thus bound the ladder approximation, we see from the work of the

TABLE IV. Monte Carlo calculations.

	$k_F\beta=1.25$				
Diagram	Value	Deviation	Diagram	Value	Deviation
I.1[a]	-9.24×10^{-1}	4.1×10^{-2}	IIA.1	-6.83×10^{-2}	1.3×10^{-3}
I.2	-3.69×10^{-2}	7.8×10^{-4}	IIA.2	1.90×10^{-2}	6.0×10^{-4}
I.3+4	-2.05×10^{-2}	6.8×10^{-4}	IIA.3	-2.32×10^{-3}	1.1×10^{-4}
I.5[b]	-3.69×10^{-2}	7.8×10^{-4}	IIA.4[b]	1.90×10^{-2}	6.0×10^{-4}
I.6	-4.84×10^{-3}	1.6×10^{-4}	IIA.5	1.26×10^{-2}	2.5×10^{-4}
IA.1	-1.79×10^{-2}	3.6×10^{-4}	IIA.6	9.60×10^{-3}	3.0×10^{-4}
IA.2	-4.48×10^{-3}	7.9×10^{-5}	III.1[a]	-2.09×10^{-1}	4.0×10^{-3}
IA.3	-1.36×10^{-2}	2.0×10^{-4}	III.2	-1.91×10^{-2}	6.6×10^{-4}
II.1	1.69×10^{-1}	5.4×10^{-3}	III.7+8[a]	1.66×10^{-1}	2.8×10^{-3}
II.2[b]	1.69×10^{-1}	5.4×10^{-3}	III.9+10	2.06×10^{-2}	5.2×10^{-4}
II.3	8.82×10^{-3}	2.6×10^{-4}	IV.1[a]	-7.99×10^{-2}	4.6×10^{-4}
II.4[a]	8.82×10^{-3}	2.6×10^{-4}	IV.2[a]	-2.41×10^{-1}	9.1×10^{-3}
II.5	3.84×10^{-2}	2.4×10^{-3}	IV.3[a]	-2.41×10^{-1}	9.1×10^{-3}
II.6	6.49×10^{-2}	3.1×10^{-3}	IV.4	4.28×10^{-2}	3.4×10^{-4}
II.7	-7.30×10^{-3}	1.5×10^{-4}	IV.5[b]	4.28×10^{-2}	3.4×10^{-4}
II.8	-1.03×10^{-2}	1.7×10^{-4}	IV.6	-1.05×10^{-2}	6.9×10^{-4}
II.9	1.81×10^{-3}	1.7×10^{-4}	IV.7[b]	-1.05×10^{-2}	6.9×10^{-4}
II.10	1.81×10^{-3}	8.0×10^{-5}	$\Sigma4$	-1.251×10^{0}	4.7×10^{-2}
II.11[b]	-1.03×10^{-2}	1.7×10^{-4}	Br 4	-1.599×10^{0}	4.5×10^{-2}
II.12[b]	-7.30×10^{-3}	1.5×10^{-4}			

[a] Included in the Brueckner approximation.
[b] Identical with a previous diagram (but must be added to find the total fourth-order coefficient).

TABLE V. [2,2] Padé approximants.

Theory	Value	Deviation
Ladder	−0.274	0.007
Brueckner	−0.258	0.006
Complete	−0.257	0.007

previous section [Eq. (3.9)], that it is sufficient for there to be no two-body bound state.

The reason that the Brueckner approximation is much closer here than the ladder approximation, in spite of the differences in the series, is readily apparent. Though the Brueckner approximation has, throughout the low to intermediate density region, about the same accuracy as has the ladder approximation, the Brueckner and complete theories cross at a density near $k_F\beta=1.25$. That this crossing is unrelated to saturation may be seen from Fig. 1 where the same crossing occurs at nearly the same density.

APPENDIX

Numerical Approximations to Θ and Φ

For $\Theta(q)$ we have used

$$\begin{aligned}\Theta(q)&=(2.2961625+4.0310705\times10^{-1}q^2+2.7742342\times10^{-2}q^4+3.6640927\times10^{-3}q^6+4.6608325\times10^{-5}q^8)\\&\quad\div(1+8.6722594\times10^{-1}q^2+3.0167356\times10^{-1}q^4+5.4870712\times10^{-2}q^6+5.6951123\times10^{-3}q^8\\&\qquad+3.3456128\times10^{-4}q^{10}+9.3739475\times10^{-6}q^{12}),\quad 0\le q\le 3\\&=(-1.9103958\times10^{1}-3.2553859\times10^{-3}q^2)\div(1-5.1016626q^2-2.3082938q^4\\&\qquad-4.5050462\times10^{-4}q^6),\quad 3<q\le 10\\&=(2.2961625+9.38826106\times10^{-1}q^2+1.284509375\times10^{-1}q^4)\div(1+1.100536551q^2+5.06906819\times10^{-1}q^4\\&\qquad+1.4627962\times10^{-1}q^6+1.55705625\times10^{-2}q^8),\quad q>10.\end{aligned}\tag{A1}$$

For $\Phi_0(q)$ we have used

$$\begin{aligned}\Phi_0(q)&=(1.8439924+8.1173867q^2+16.263688q^4+15.731397q^6+5.0831540q^8+0.39386421q^{10})\\&\quad\div(1+6.2859062q^2+17.968033q^4+28.926281q^6+26.455817q^8+12.907287q^{10}+3.0140573q^{12}\\&\qquad+0.31234636q^{14}),\quad 0\le q\le 2\\&=(4.0781999\times10^{-1}+2.1038983\times10^{-3}q^2-1.3740016\times10^{-5}q^4)\div(1-3.2366615\times10^{-2}q^2+2.8222651\times10^{-1}q^4\\&\qquad+1.5111686\times10^{-3}q^6-9.7225146\times10^{-6}q^8),\quad 2<q\le 15\\&=(1.8439924+0.3251992159q^2)\div(1+2.06019055q^2+1.1876602113q^4+0.2280375132q^6),\quad 15<q.\end{aligned}\tag{A2}$$

For $\Phi_2(q)$ we have used

$$\begin{aligned}\Phi_2(q)&=q^2[(1.9307396+4.7397050q^2+6.9503809q^4+2.4114265q^6)\div(1+6.5398428q^2+19.991277q^4\\&\quad+36.171749q^6+40.746141q^8+28.205082q^{10}+11.33242q^{12}+2.3412168q^{14}+0.1986048q^{16})]^{1/2},\quad 0\le q\le 2\\&=[(1.7841509\times10^{-1}+1.7038724\times10^{-3}q^2-4.7815722\times10^{-6}q^4\div(1+3.0102673\times10^{-1}q^2\\&\quad+1.5205565\times10^{-1}q^4+1.5396959\times10^{-2}q^6+9.6045890\times10^{-5}q^8-2.9892311\times10^{-7}q^{10})]^{1/2},\quad 2<q\le 15\\&=q^2[(1.9307396+9.413756495\times10^{-3}q^2+1.551145537\times10^{-6}q^4)\div(1+4.089853626q^2+6.383272234q^4\\&\quad+4.627314251q^6+1.476156636q^8+1.498720163\times10^{-1}q^{10}+5.776466272\times10^{-4}q^{12}\\&\qquad+9.09971649\times10^{-8}q^{14})]^{1/2},\quad q>15.\end{aligned}\tag{A3}$$